Aspirin-triggered lipoxin inhibits atherosclerosis progression in ApoE$^{-/-}$ mice

Marcelo H Petri[1], Andrés Laguna-Fernandez[1], Hildur Arnardottir[1], Craig E Wheelock[2], Mauro Perretti[3], Göran K Hansson[1] and Magnus Bäck[1,4]

[1]Experimental Cardiovascular Research Group, Cardiovascular Medicine Unit, Center for Molecular Medicine, Department of Medicine, Karolinska Institutet, Stockholm, Sweden, [2]Department of Medical Biochemistry and Biophysics, Karlinska Institutet, Stockholm, Sweden, [3]William Harvey Research Institute, Barts and The London School of Medicine, Queen Mary University of London, London, United Kingdom, and [4]Department of Cardiology, Karolinska University Hospital, Stockholm, Sweden

Corresponding author: Magnus Bäck
Translational Cardiology
Center for Molecular Medicine
L8:03
Karolinska University Hospital
171 76 Stockholm, Sweden
E-mail: Magnus.Back@ki.se
Tel: +46-8-51770000
Fax: +46-8-333147

Word count (excl Introduction, Methods and References)**:** 2883 words

Abstract word count: 242 words

No. of Tables: 4

No. of Figures: 6

This article has been accepted for publication and undergone full peer review but has not been through the copyediting, typesetting, pagination and proofreading process which may lead to differences between this version and the Version of Record. Please cite this article as doi: 10.1111/bph.13707

Running title: ATL reduces atherosclerosis

Abbreviations

ApoE	apolipoprotein E
ATL	aspirin-triggered lipoxin A_4
HFD	high fat diet
HPRT	hypoxanthine phosphoribosyl-transferase
IL	interleukin
Ldlr	low density lipoprotein receptor
MMP	matrix metallopeptidase
OCT	optimal cutting temperature
RvD1	resolvin D1

Table of links

GPCR:

ALX/FPR2

http://www.guidetopharmacology.org/GRAC/ObjectDisplayForward?objectId=223

Ligand:

Aspirin triggered lipoxin A_4

http://www.guidetopharmacology.org/GRAC/LigandDisplayForward?ligandId=3933

Abstract

Background and Purpose. Atherosclerosis is characterized by a chronic non-resolving inflammation in the arterial wall. Aspirin-triggered lipoxin A_4 (ATL) is a potent anti-inflammatory mediator, involved in the resolution of inflammation. However, the therapeutic potential of immune targeting by means of ATL in atherosclerosis has not previously been explored. The aim of the present study was to determine the effects of ATL and its receptor Fpr2 on atherosclerosis development and progression in apolipoprotein E ($ApoE^{-/-}$) deficient mice.

Experimental Approach. $ApoE^{-/-}xFpr2^{+/+}$ and $ApoE^{-/-}xFpr2^{-/-}$ mice were generated. Four weeks old mice were fed a high fat diet for 4 weeks and 16 weeks old mice fed chow diet received osmotic pumps containing either vehicle or ATL for 4 weeks. Atherosclerotic lesion size and cellular composition was measured in the aortic root and thoracic aorta. Lipid levels and leukocyte counts were measured in blood and mRNA was isolated from abdominal aorta and spleen.

Key Results. ATL blocked atherosclerosis progression in the aortic root and thoracic aorta of $ApoE^{-/-}$ mice. In addition, ATL reduced macrophage infiltration and apoptotic cells in atherosclerotic lesions. The mRNA levels of several cytokines and chemokines in spleen and aorta were reduced by ATL, whereas circulating leukocyte levels were unchanged. The ATL-induced athero-protection was absent in $ApoE^{-/-}$ mice lacking the Fpr2 receptor.

Conclusion and Implications. ATL blocked atherosclerosis progression by means of an Fpr2-mediated reduced local and systemic inflammation. These results suggest a therapeutic potential for this anti-inflammatory and pro-resolving agent in atherosclerosis.

Introduction

Inflammation plays a well-established role in the initiation and progression of atherosclerosis, and may represent an important therapeutic target in cardiovascular prevention (Libby *et al.*, 2011). Most of the evaluated treatment options, for example blocking inflammatory mediators and the induction of immunoregulatory responses, aim to inhibit the pro-inflammatory signaling in atherosclerotic lesions (Bäck & Hansson, 2015). In addition to a continued stimulation of inflammation, chronic inflammation is also favored by a failure in the resolution of inflammation (Serhan, 2014). As an example, a defective uptake of apoptotic cells (efferocytosis) increases experimental atherosclerosis (Thorp *et al.*, 2008; Van Vre *et al.*, 2012).

The lipoxygenase metabolism of arachidonic acid yields the pro-inflammatory mediators leukotrienes. Targeting the specific leukotriene receptors reduces atherosclerosis and intimal hyperplasia in different animal models (Bäck *et al.*, 2005; Ketelhuth *et al.*, 2015). In addition, anti-leukotrienes used in the treatment of asthma have been associated with decreased cardiovascular risk in observational studies (Ingelsson *et al.*, 2012), hence reinforcing the potent pro-inflammatory and pro-atherogenic role of this class of lipid mediators. On the other hand, dual lipoxygenation of arachidonic acid yields a group of lipid mediators called lipoxins (Serhan, 1997; Serhan, 2014), which have the opposite effects to leukotrienes. Lipoxins have been shown to induce a resolution of inflammation, by means of for example stimulating efferocytosis (Maderna *et al.*, 2010), granulocyte apoptosis (Barnig *et al.*, 2013), leukocyte egress (van Gils *et al.*, 2012) modulate endothelial activation and reduce leukocyte recruitment after ischemia/reperfusion (Brancaleone *et al.*, 2013; Smith *et al.*, 2015). In addition, the 15-epimer of lipoxin A_4, referred to as aspirin-triggered lipoxin A_4 (ATL) due to the stimulation of its formation by aspirin-induced cyclooxygenase acetylation (Serhan, 1997), reduces smooth muscle cell responses *in vitro* and intimal hyperplasia after

carotid ligation in mice *in vitro* (Petri *et al.*, 2015). However, the therapeutic potential of ATL in atherosclerosis has remained unexplored.

Lipoxin A_4 and ATL share their signaling pathway by means of the FPR2/ALX receptor (Bäck *et al.*, 2014) with other both pro-inflammatory (*e.g.* amyloid and antibacterial peptides (Ye *et al.*, 2009)), and pro-resolving mediators, such as annexin A1 (Hayhoe *et al.*, 2006) and resolvin D1 (RvD1) (Krishnamoorthy *et al.*, 2012). Three major cell types within human atherosclerotic lesions express FPR2/ALX, namely macrophages, vascular smooth muscle cells and endothelial cells (Petri *et al.*, 2015). In atherosclerosis-prone low density lipoprotein receptor deficient ($Ldlr^{-/-}$) mice, pro-inflammatory ligands for the murine homologue of FPR2/ALX (termed Fpr2) appear to dominate to promote leukocyte recruitment and activation in atherosclerotic lesions (Petri *et al.*, 2015). Increased atherosclerotic lesion size has also been reported in hyperlipidemic $Fpr2^{-/-}$ mice at early time-points, associated with defective pro-resolving signaling of the FPR2/ALX peptide agonist annexin A1 (Drechsler *et al.*, 2015). Although FPR2/ALX signaling apparently is activated in atherosclerosis, the effects of ATL as a pro-resolving mediator and a possible therapeutic molecule for the treatment of atherosclerosis have not previously been evaluated.

The aim of the present study was to unravel the potential therapeutic value of ATL in atherosclerosis, and to explore the mechanisms involved, in terms of receptor activation and key local and systemic pro-atherogenic processes during initiation and progression of the disease.

Methods

Generation of ApoE and Fpr2 double knock-out mice

All experiments were performed according to the animal regulations and guidelines of Karolinska Institutet (ethical permit #N138/12). Fpr2 deficient mice were generated at the

William Harvey Institute (London, UK) as previously described through insertion of the gene cassette and a GFP reporter in reverse orientation into intron 1 of Fpr2, which prevented transcriptional read-through of the Fpr2 as well as Fpr3 genes (Dufton *et al.*, 2010). Therefore, these mice have also been termed Fpr2/Fpr3 knock-out mice (Brancaleone *et al.*, 2013), but will be referred to as $Fpr2^{-/-}$ in the present report. The mice were backcrossed for at least 7 generations in to a C57BL/6 background before been crossed to $ApoE^{-/-}$ mice from Taconic (Ry, Denmark) for another 2 generations to achieve $ApoE^{-/-}$ x $Fpr2^{-/-}$ mice. Female mice were kept in 12 hours cycle light/dark with either chow diet (D12102, Research Diets Inc, New Brunswick, NJ) or high fat diet (HFD, 21% fat, D12108C, Research Diets Inc, New Brunswick, NJ) and water *ad libitum*.

ATL treatment protocol

In a first set of experiments, 4 groups of mice were studied. $ApoE^{-/-}xFpr2^{+/+}$ and $ApoE^{-/-}xFpr2^{-/-}$ mice were subjected to osmotic pump (Alzet Mod #2004) implantation under general anesthesia (1.5% isoflurane; 1 L/min) at 16 weeks of age. Mice were randomized to receive osmotic pumps loaded with either vehicle (15% of ethanol) or ATL (10μg/kg; Millipore) as previously described (Petri, Laguna-Fernandez, Tseng, Hedin, Perretti & Bäck, 2015). The skin was sutured with 5-0 Vicryl and 0.1% of buprenorphine injected S.C. at the moment of the pump implantation and every morning for the next 2 days. The mice were kept on chow diet during the whole experiment until sacrifice. After euthanasia by CO_2, a blood sample was withdrawn by cardiac puncture and the heart, spleen, and aorta were harvested.

In a second set of experiments, 3 groups of $ApoE^{-/-}xFpr2^{+/+}$ mice were studied. The first group was sacrificed at 16 weeks of age, representing the baseline before the treatment protocols began. The remaining 16 week-old mice were subjected to osmotic pump implantation and randomized to the same treatment protocols as indicated above, to obtain a

replication of the findings and to decipher if ATL treatment either reduced progression or induced regression of atherosclerotic lesions.

In a third set of experiments, 4 week old $ApoE^{-/-}xFpr2^{+/+}$ and $ApoE^{-/-}xFpr2^{-/-}$ mice were fed a high fat diet and sacrificed after 4 weeks to study the genotype-induced effect on atherosclerosis initiation.

ATL analysis

Osmotic pumps filled with ATL were incubated at 37 degrees for 4 weeks, and the content was then collected and 2 volumes of ice-cold MeOH was added followed by C18 solid phase extraction for liquid chromatography and tandem mass spectrometry (LC-MS-MS; Colas *et al.*, 2014; Stanke-Labesque *et al.*, 2012). The system consisted of Waters Xevo ® TQS triple quadruple equipped with Acquity UPLC System from Waters Corporation and autosampler cooled to 5˚C (Milford, MA, USA). An Acquity UPLC BEH (Ethylene Bridged Hybrid) C18 column (130 Å, 1.7 um, 2.1 mm x 150 mm) equipped with a pre-column (Acquity UPLC C18 VanGuard Pre-column, 130 Å, 1.7um, 2.1 mm x 5 mm; Milford, US) was used with gradients A (0.1% acetic acid in water) and B (acetonitrile/isopropanol; 90:10 (v/v)) from 80:20 (v/v) to 0:100 (v/v) in 17 min at a 0.5 ml/min flow rate which was then equilibrated to initial conditions 2.5 min. Data acquisition was performed in negative ionization mode, and identification conducted in accordance with published criteria (Colas *et al.*, 2014) with a minimum of six diagnostic ions.

Blood and plasma analysis

Circulating leukocytes were measured by an automated cell counter (ABC vetpack). Cholesterol and triglycerides were measured in plasma by kits from Randox following the manufacturer's protocol. Protein quantification was performed by ELISA following the

manufacturer's protocols; IL-6 (Cat # 431303, BioLegend), MMP13 (cat# LS-F5519, LSBio) and serum amyloid A (SAA; Cat# KMA0021, Invitrogen).

Evaluation of atherosclerosis

The thoracic aorta was opened longitudinally, pinned, and stained with Sudan IV solution. A micrograph of the aortic arch was captured using a Leica Microsystems color video camera, and the image analysis was performed using ImageJ in a blinded fashion. The area of the aortic arch covered by atherosclerotic lesions divided by the aortic arch area was calculated as previously described (Petri *et al.*, 2015).

In addition, the upper portion of the heart and aortic root was embedded in Optimal Cutting Temperature (OCT) compound, and frozen at -80°C. Serial 10-µm cryosections were collected beginning at the aortic valve cusp for a distance of 800 µm. Oil red-O staining was performed on eight formalin-fixed sections collected every 100 µm from the aortic valve cusps. Lesion area was determined in a blinded fashion by light microscopy using Leica Qwin. The mean value of lipid stained areas (lesion size) of aortic root sections was calculated.

Immunohistochemistry and plaque composition analysis

Antibodies against CD68 (MCA1957, Serotec) and CD4 (553647, BD) were used for the immunodetection of macrophages and T-cells in sections representing the largest lesion area of each aortic root. One section per animal was analyzed, and N indicates the number of animals. In a subset of animals, four sections from each aortic root were stained for CD68, CD4, and apoptosis detection and yielded similar results as those obtained at the largest lesion size (data not shown). Biotinylated secondary antibodies and Nova Red staining were used to identify positive cells/areas, and sections were counterstained with hematoxylin.

Apoptotic cells were detected using an *in situ* apoptosis detection kit (ab206386, Abcam) following the manufacturer's protocol. For collagen quantification, sections were stained with Picrosirius red (Histolab® HL27150) and analyzed under polarized light for the amount of red (thick) and green (thin) fibers quantified by Leica Qwin. The slides were mounted and the sections were analyzed as described for oil red-O for quantification of CD68, CD4 and apoptosis detection positive areas.

Real-Time PCR

Total RNA was isolated from abdominal aorta and spleen using QIAZOL (Qiagen) and concentrations were measured spectrophotometrically using Nanodrop 1000 (Thermo Fisher Scientific). Reverse-transcription was performed with high capacity kit (Life Technologies, USA). Real time PCR was performed on a 7900HT Fast Real-Time PCR system (Perkin-Elmer Applied Biosystems) using TaqMan Assay-on-Demand from Applied Biosystems for interleukin (IL) 6 (Mm00446190_m1), matrix metallopeptidase (MMP) 13 (Mm00439491_m1), CCL2 (Mm00441242_m1), CCL5 (Mm01302427_m1), CXCL16 (Mm00469712_m1), interferon (IFN) γ (Mm01168134_m1), IL-23a (Mm00518984_m1), SAA (Mm00441203_m1), and tumor necrosis factor (TNF ; Mm00443258_m1). Results are expressed as $2^{-\Delta CT}$ obtained by comparing obtained by comparing the threshold cycle (CT) for the gene of interest with that obtained using hypoxanthine phosphoribosyl-transferase hypoxanthine phosphoribosyl-transferase (HPRT; Mm01545399_m1) as housekeeping gene.

Data and statistical analysis

Data are expressed as mean ± standard error of the mean (SEM). When comparing two groups, either a Student´s t-test or Mann-Whitney U test were used after normality test was performed. Either a one or two way ANOVA was used for multiple comparisons as indicated,

followed by a Dunnett's test versus control. A $P<0.05$ was considered significant. All analyses were performed using SigmaPlot version 12.5 (Systat Software Inc).

Results

ATL stability

The stability of ATL was assessed and the results are shown in Fig 1. ATL remained intact following 4 weeks incubation in osmotic pump at 37˚C, with only small amount (<10%) of potential isomerization as observed by appearance of additional peaks (Fig. 1). Its retention time (5.70 min) and MS-MS spectra was identical to that of the 15-epi-LXA_4 synthetic standard. Furthermore, it retained its tetraene chromophore with λ_{max} at 300 nm and shoulders at 287 and 315 nm, identical to that of the 15-epi-LXA_4 standard (data not shown).

ATL block atherosclerosis progression by means of Fpr2

To study the therapeutic potential of ATL on established disease, 16 weeks old $ApoE^{-/-}xFpr2^{-/-}$ and $ApoE^{-/-}xFpr2^{+/+}$ mice were randomized to treatment with either vehicle or ATL for 4 weeks followed by atherosclerosis assessment. At the end of the treatment period, ATL-treated $ApoE^{-/-}xFpr2^{+/+}$ mice exhibited significantly reduced atherosclerosis burden compared with vehicle-treated mice, both at the aortic root level (Fig 2A) and *en face* analysis of the aortic arch (Fig 2B). Furthermore, vehicle-treated $ApoE^{-/-}xFpr2^{-/-}$ mice exhibited reduced lesion size at both locations compared with vehicle-treated $ApoE^{-/-}xFpr2^{+/+}$ mice (Fig 2A and 2B). In contrast, atherosclerotic lesion size was not altered by ATL treatment in $ApoE^{-/-}xFpr2^{-/-}$ mice. There were no significant differences in lipid levels, blood cell counts or body weights between the different groups (Table 1).

To clarify if ATL either regressed or inhibited the progression of atherosclerosis, the treatment protocol was repeated in another series of $ApoE^{-/-}xFpr2^{+/+}$ mice in which the

atherosclerotic lesion size after 4 weeks of either ATL or vehicle treatment was compared with that observed in littermate mice sacrificed at 16 weeks of age, which corresponded to the start of the treatments. After four weeks treatment with vehicle, 20 week old mice exhibited significantly increased atherosclerotic lesions in both the aortic root (Fig 3A) and aortic arch (Fig 3B) as compared with the 16 week old mice at baseline. In contrast, no significant differences compared with baseline were observed after 4 weeks ATL treatment, indicating that ATL prevented plaque progression in both the aortic root and aortic arch (Fig 3). ATL did not significantly alter lipids, blood cell counts or body weight of 20 week old mice (Table 2).

ATL alters plaque composition

The analysis of the atherosclerotic plaque composition in the aortic root of $ApoE^{-/-}xFpr2^{+/+}$ mice receiving either ATL or vehicle is shown in Fig 4. Mice receiving ATL exhibited less CD68 positive area compared with vehicle-treated mice (Fig 4A), whereas there were no significant differences in the amount of CD4 positive cells between ATL and vehicle-treatment (Fig 4B). In addition, the amount of apoptotic cells were reduced on the ATL treated mice (Fig 4C). The collagen content, as assessed by Picrosirius red staining revealed a larger proportion of thick collagen fibers (stained in red) in ATL-treated mice (Fig 4D).

Atherosclerosis initiation is Fpr2 independent.

In order to clarify whether Fpr2 signaling was important for the initiation of atherosclerosis, 4 weeks old $ApoE^{-/-}xFpr2^{-/-}$ and $ApoE^{-/-}xFpr2^{+/+}$ mice were fed a HFD for 4 weeks. No differences were observed between the two genotypes in terms of atherosclerotic lesion size (Fig 5), lipid levels or blood count (Table 3).

ATL reduced systemic inflammation Fpr2 dependently

In order to address whether the observed ATL-induced effects were limited to the vasculature, or if they were observed systemically, gene expression profiles were compared between the aorta and the spleen. ATL-treated mice exhibited significantly lower levels of a number of cytokines and chemokines in both the aorta and the spleen, as indicated in Table 4. Further examples of the anti-inflammatory effects of ATL are shown in Fig 6, namely the decreased levels of IL-6 and MMP-13 mRNA in the spleen and the aorta and their concomitant decreased circulating protein levels in plasma (Fig 6). In contrast, ATL did not significantly reduce the IL-6 and MMP-13 mRNA levels in organs derived from $ApoE^{-/-}$ $xFpr2^{-/-}$ mice (data not shown), supporting that the anti-inflammatory effects of ATL requires a functional Fpr2 signaling. Finally, SAA, another proinflammatory mediator, which is also a Fpr2 agonist also exhibited significantly reduced mRNA levels in the aorta (Fig 6G) and the spleen (Fig 6H) in response to ATL-treatment, and a trend towards lower circulating protein levels in SAA-treated mice (Fig 6I)

Discussion

The present study raises the notion of a therapeutic potential for ATL in stopping the progression of established atherosclerosis. Furthermore, we show that the effects of ATL were transduced by means of Fpr2, reducing vascular inflammation in terms of for example lowering the number of plaque macrophages and inhibiting proinflammatory gene expression. We also show that ATL promoted less systemic inflammation. Taken together, these results suggest that ATL treatment could represent a novel therapeutic strategy to prevent atherosclerosis progression.

Whereas the inhibitory effects of ATL on acute inflammation, such as inflammatory cell recruitment in inflamed dorsal air pouches (Dufton *et al.*, 2010) and microvascular

dysfunction after ischemia-reperfusion (Brancaleone *et al.*, 2013; Vital *et al.*, 2016) are well established, its role for resolving chronic inflammation has been less extensively explored. Long term ATL treatment to mice by means of osmotic pumps has however been established to reveal that this lipid mediator reduces intimal hyperplasia after carotid artery ligation (Petri *et al.*, 2015). Adopting the latter therapeutic strategy, the present study demonstrates the stability of ATL administered under those conditions and for the first time reveals that 4 weeks ATL treatment of ApoE-deficient mice with established atherosclerosis significantly reduced lesion size in the aortic root and arch compared with vehicle-treated mice.

The ATL-induced effects on atherosclerosis were observed in the absence of significant alterations of the plasma lipid profile, suggesting that pro-inflammatory pathways rather than lipid metabolism were targeted by this treatment. In line with this, a reduced number of macrophages were observed in atherosclerotic lesions derived from ATL-treated mice compared with vehicle-treated mice, whereas lesion T-lymphocyte infiltration was not altered by ATL. Macrophages in human atherosclerotic lesions indeed express the ATL receptor FPR2/ALX (Petri *et al.*, 2015), and lipoxin stimulation of human and murine myeloid cells reduces inflammation *in vivo* and *in vitro* (Devchand *et al.*, 2003; Maderna *et al.*, 2010; Petri *et al.*, 2015; Wu *et al.*, 2011). Efferocytosis by macrophages is enhanced by lipoxins (Godson *et al.*, 2000) and inhibited in $Fpr2^{-/-}$ mice (Petri *et al.*, 2015), suggesting that ATL-induced efferocytosis by means of Fpr2 signaling may contribute to its athero-protective effects. In support of the latter, a reduced number of apoptotic cells were observed in atherosclerotic lesions derived from ATL-treated mice in the present study. An increased proportion of thick collagen fibers were also observed in atherosclerotic lesions after ATL-treatment, which is line with previous findings in $Fpr2^{-/-}$ mice (Petri *et al.*, 2015) and supports that ATL in addition may induce a more stable lesion phenotype, which is further reinforced by the decrease in the collagenase MMP-13 after ATL treatment in the present study.

These beneficial effects of ATL were reproduced in a second series of mice, in which the atherosclerotic lesion size at 20 weeks after 4 weeks osmotic pump ATL treatment was unchanged compared with that observed in 16 week old mice sacrificed at the start of the treatment period. Based on the latter experiments, we can conclude that ATL treatment blocked the significant progression of atherosclerosis, which was observed in vehicle-treated mice. It is also important to stress that the mice had atherosclerotic plaques when treatment was initiated, hence extending previous observations that the Fpr2 agonist Annexin A1 prevented atherosclerosis development in younger ApoE knock-out mice fed a HFD (Drechsler *et al.*, 2015).

Studies in other animal models have shown that lipoxin-induced effects are abolished in mice lacking the murine FPR2/ALX orthologue Fpr2 (Brancaleone *et al.*, 2013; Dufton *et al.*, 2010; Petri *et al.*, 2015; Vital *et al.*, 2016). To address the signaling pathways involved in the observed reduction of atherosclerosis induced by ATL, we generated ApoE and Fpr2 double knock-out mice for the present study. Importantly, ATL-treatment was ineffective in reducing atherosclerosis in $ApoE^{-/-}$ mice lacking Fpr2. The latter finding hence indicate that Fpr2 is the receptor exclusively mediating the beneficial effects of ATL in terms of atherosclerosis development.

Another important finding that emerged from the latter analysis was that Fpr2-deficient $ApoE^{-/-}$ mice exhibited reduced atherosclerosis. Those results confirm our previous results in Ldlr and Fpr2 double knock-out mice at similar time points and lesion sizes (Petri *et al.*, 2015). The similar results obtained by Fpr2 deletion in two different murine atherosclerosis models strongly reinforces the notion that pro-inflammatory Fpr2 agonists prevail the anti-inflammatory receptor ligands in atherosclerosis. Indeed, our previous study showed low levels of lipoxins in $Ldlr^{-/-}$ mice fed a high fat diet compared with the proinflammatory Fpr2 ligand SAA (Petri *et al.*, 2015). Taken together, those observations

supports that murine atherosclerosis models are associated with low pro-resolving Fpr2 agonists, which may contribute to a failure in the resolution of inflammation. Interestingly, ATL-treatment decreased the levels of the SAA levels in the present study, hence potentially further facilitating its proresolving Fpr2 signaling.

The lack of effects at early stages of atherosclerosis development in the present study are in contrast to a study using a different Fpr2 gene targeting strategy, which reported exacerbated atherosclerosis in $ApoE^{-/-}$ mice after 4 weeks of HFD (Drechsler *et al.*, 2015). While it remains to be established whether the different Fpr2 genetic targeting techniques or other experimental conditions accounted for those differential results, it should be pointed out that the results of the present study are in line with previous findings that did not reveal any significant effects of Fpr2 deletion at early stages of atherosclerosis in either $Ldlr^{-/-}$ mice (Petri *et al.*, 2015) or after bone marrow transplantation of $Fpr2^{-/-}$ bone marrow to $Ldlr^{-/-}$ mice (Fredman *et al.*, 2015).

Taken together with the above-mentioned reports, the results of the present study support that ATL treatment enhances the resolution of inflammation and inhibits the development of atherosclerosis. In support of the latter, a failure in the resolution of inflammation in terms of reduced lipoxin levels has indeed been established in both experimental atherosclerosis (Petri *et al.*, 2015) and clinical biomarker studies (Ho *et al.*, 2010). Although not specifically addressed in the present study, it should be noted that aspirin enhances ATL production in atherosclerosis (Brezinski *et al.*, 1992; Ho *et al.*, 2010), and it can hence be anticipated that ATL production may represent an additional beneficial effect of aspirin in cardiovascular prevention, which goes beyond its anti-aggregatory effects on platelets.

As a final approach in the present study, we sought to determine whether the observed Fpr2-mediated reduction in atherosclerosis and lesion macrophage content induced

by ATL solely represented a local vascular response, or if systemic inflammation was also altered in ATL-treated mice. Based on the lack of significant alterations of the peripheral white blood cell count, we conclude that no apparent myeloid dysfunction was induced by ATL. Nevertheless, ATL reduced expression levels of a number of proinflammatory cytokines, chemokines and enzymes in both the spleen and the aorta, supporting that ATL decreased systemic inflammation. This observation is supported by the decreased circulating proteins levels of Il-6 and MMP-13.

In summary, ATL treatment initiated at already established atherosclerosis stopped the progression of disease over 4 weeks. These effects of ATL were absent in mice lacking Fpr2, the murine orthologue of the human FPR2/ALX receptor, supporting that the beneficial effects of ATL on atherosclerosis are mediated through this signaling pathway. In the absence of ATL, Fpr2 deficiency however protected against atherosclerosis progression, supporting the notion of a failure in the resolution of inflammation, which can be overrun by the treatment of atherosclerotic mice with the proresolving mediator ATL. This is further supported by the reduced macrophage infiltration and inflammatory mRNA levels in ATL-treated mice. In conclusion, stopping atherosclerosis progression by means of the ATL and FPR2/ALX pathway may represent a novel therapeutic option for immune targeting in cardiovascular prevention.

Conflicts of interest

None declared

Acknowledgements

The Authors would like to acknowledge Jessica Lundgren, Selameyhune Assefa, Sandra Olsson and Ann-Christine Eklöf for the valuable support in the animal facility.

Funding

This work was supported by the Swedish Research Council (Grant number 2014-2312); the Swedish Heart and Lung Foundation (grant numbers 20150600 and 20150683) and the Stockholm County Council (grant number 20140222). Mauro Perretti was supported by the Wellcome Trust Programme (grant number 086867/Z/08/Z). Marcelo Heron Petri was supported by a KID PhD-fellowship from Karolinska Institutet.

Author contributions

MHP, ALF, and MB planned and conceived the study. MHP, ALF and HA performed the experiments. MHP, ALF, HA, CEW, and MB performed the data analysis. MHP and MB wrote the manuscript and ALF, HH, MP, CEW, and GKH revised it critically for important intellectual content.

References

Barnig C, Cernadas M, Dutile S, Liu X, Perrella MA, Kazani S*, et al.* (2013). Lipoxin A4 regulates natural killer cell and type 2 innate lymphoid cell activation in asthma. Sci Transl Med 5**:** 174ra126.

Brancaleone V, Gobbetti T, Cenac N, le Faouder P, Colom B, Flower RJ*, et al.* (2013). A vasculo-protective circuit centered on lipoxin A4 and aspirin-triggered 15-epi-lipoxin A4 operative in murine microcirculation. Blood 122**:** 608-617.

Brezinski DA, Nesto RW, & Serhan CN (1992). Angioplasty triggers intracoronary leukotrienes and lipoxin A4. Impact of aspirin therapy. Circulation 86**:** 56-63.

Bäck M, Bu DX, Branstrom R, Sheikine Y, Yan ZQ, & Hansson GK (2005). Leukotriene B4 signaling through NF-kappaB-dependent BLT1 receptors on vascular smooth muscle cells in atherosclerosis and intimal hyperplasia. Proc Natl Acad Sci U S A 102**:** 17501-17506.

Bäck M, & Hansson GK (2015). Anti-inflammatory therapies for atherosclerosis. Nat Rev Cardiol 12**:** 199-211.

Bäck M, Powell WS, Dahlen SE, Drazen JM, Evans JF, Serhan CN*, et al.* (2014). Update on leukotriene, lipoxin and oxoeicosanoid receptors: IUPHAR Review 7. British journal of pharmacology 171**:** 3551-3574.

Colas RA, Shinohara M, Dalli J, Chiang N, & Serhan CN (2014). Identification and signature profiles for pro-resolving and inflammatory lipid mediators in human tissue. Am J Physiol Cell Physiol 307**:** C39-54.

Devchand PR, Arita M, Hong S, Bannenberg G, Moussignac RL, Gronert K*, et al.* (2003). Human ALX receptor regulates neutrophil recruitment in transgenic mice: roles in inflammation and host defense. FASEB journal : official publication of the Federation of American Societies for Experimental Biology 17**:** 652-659.

Drechsler M, de Jong R, Rossaint J, Viola JR, Leoni G, Wang JM*, et al.* (2015). Annexin A1 counteracts chemokine-induced arterial myeloid cell recruitment. Circ Res 116**:** 827-835.

Dufton N, Hannon R, Brancaleone V, Dalli J, Patel HB, Gray M*, et al.* (2010). Anti-inflammatory role of the murine formyl-peptide receptor 2: ligand-specific effects on leukocyte responses and experimental inflammation. Journal of immunology 184**:** 2611-2619.

Fredman G, Kamaly N, Spolitu S, Milton J, Ghorpade D, Chiasson R*, et al.* (2015). Targeted nanoparticles containing the proresolving peptide Ac2-26 protect against advanced atherosclerosis in hypercholesterolemic mice. Sci Transl Med 7**:** 275ra220.

Godson C, Mitchell S, Harvey K, Petasis NA, Hogg N, & Brady HR (2000). Cutting edge: lipoxins rapidly stimulate nonphlogistic phagocytosis of apoptotic neutrophils by monocyte-derived macrophages. Journal of immunology 164**:** 1663-1667.

Hayhoe RP, Kamal AM, Solito E, Flower RJ, Cooper D, & Perretti M (2006). Annexin 1 and its bioactive peptide inhibit neutrophil-endothelium interactions under flow: indication of distinct receptor involvement. Blood 107**:** 2123-2130.

Ho KJ, Spite M, Owens CD, Lancero H, Kroemer AH, Pande R*, et al.* (2010). Aspirin-triggered lipoxin and resolvin E1 modulate vascular smooth muscle phenotype and correlate with peripheral atherosclerosis. Am J Pathol 177**:** 2116-2123.

Ingelsson E, Yin L, & Back M (2012). Nationwide cohort study of the leukotriene receptor antagonist montelukast and incident or recurrent cardiovascular disease. J Allergy Clin Immunol 129**:** 702-707 e702.

Ketelhuth DF, Hermansson A, Hlawaty H, Letourneur D, Yan ZQ, & Back M (2015). The leukotriene B receptor (BLT) antagonist BIIL284 decreases atherosclerosis in ApoE mice. Prostaglandins & other lipid mediators.

Krishnamoorthy S, Recchiuti A, Chiang N, Fredman G, & Serhan CN (2012). Resolvin D1 receptor stereoselectivity and regulation of inflammation and proresolving microRNAs. Am J Pathol 180**:** 2018-2027.

Libby P, Ridker PM, & Hansson GK (2011). Progress and challenges in translating the biology of atherosclerosis. Nature 473**:** 317-325.

Maderna P, Cottell DC, Toivonen T, Dufton N, Dalli J, Perretti M*, et al.* (2010). FPR2/ALX receptor expression and internalization are critical for lipoxin A4 and annexin-derived peptide-stimulated phagocytosis. FASEB journal : official publication of the Federation of American Societies for Experimental Biology 24**:** 4240-4249.

Petri MH, Laguna-Fernandez A, Gonzalez-Diez M, Paulsson-Berne G, Hansson GK, & Bäck M (2015). The role of the FPR2/ALX receptor in atherosclerosis development and plaque stability. Cardiovasc Res 105**:** 65-74.

Petri MH, Laguna-Fernandez A, Tseng CN, Hedin U, Perretti M, & Bäck M (2015). Aspirin-triggered 15-epi-lipoxin A(4) signals through FPR2/ALX in vascular smooth muscle cells and protects against intimal hyperplasia after carotid ligation. Int J Cardiol 179**:** 370-372.

Serhan CN (1997). Lipoxins and novel aspirin-triggered 15-epi-lipoxins (ATL): a jungle of cell-cell interactions or a therapeutic opportunity? Prostaglandins 53**:** 107-137.

Serhan CN (2014). Pro-resolving lipid mediators are leads for resolution physiology. Nature 510**:** 92-101.

Smith HK, Gil CD, Oliani SM, & Gavins FN (2015). Targeting formyl peptide receptor 2 reduces leukocyte-endothelial interactions in a murine model of stroke. FASEB journal : official publication of the Federation of American Societies for Experimental Biology.

Stanke-Labesque F, Pepin JL, de Jouvencel T, Arnaud C, Baguet JP, Petri MH*, et al.* (2012). Leukotriene B4 pathway activation and atherosclerosis in obstructive sleep apnea. J Lipid Res 53**:** 1944-1951.

Thorp E, Cui D, Schrijvers DM, Kuriakose G, & Tabas I (2008). Mertk receptor mutation reduces efferocytosis efficiency and promotes apoptotic cell accumulation and plaque necrosis in atherosclerotic lesions of apoe-/- mice. Arterioscler Thromb Vasc Biol 28**:** 1421-1428.

van Gils JM, Derby MC, Fernandes LR, Ramkhelawon B, Ray TD, Rayner KJ*, et al.* (2012). The neuroimmune guidance cue netrin-1 promotes atherosclerosis by inhibiting the emigration of macrophages from plaques. Nat Immunol 13**:** 136-143.

Van Vre EA, Ait-Oufella H, Tedgui A, & Mallat Z (2012). Apoptotic cell death and efferocytosis in atherosclerosis. Arterioscler Thromb Vasc Biol 32**:** 887-893.

Vital SA, Becker F, Holloway PM, Russell J, Perretti M, Granger DN*, et al.* (2016). Fpr2/ALX Regulates Neutrophil-Platelet Aggregation and Attenuates Cerebral Inflammation: Impact for Therapy in Cardiovascular Disease. Circulation.

Wu J, Wang A, Min Z, Xiong Y, Yan Q, Zhang J*, et al.* (2011). Lipoxin A4 inhibits the production of proinflammatory cytokines induced by beta-amyloid in vitro and in vivo. Biochemical and biophysical research communications 408**:** 382-387.

Ye RD, Boulay F, Wang JM, Dahlgren C, Gerard C, Parmentier M*, et al.* (2009). International Union of Basic and Clinical Pharmacology. LXXIII. Nomenclature for the formyl peptide receptor (FPR) family. Pharmacological reviews 61**:** 119-161.

Table 1: Lipid levels and white blood cell counts (mean±SEM) for ApoE$^{-/-}$ x Fpr2$^{+/+}$ and ApoE$^{-/-}$ x Fpr2$^{-/-}$ treated with either Vehicle or ATL.

	ApoE$^{-/-}$ x Fpr2$^{+/+}$		***ApoE$^{-/-}$ x Fpr2$^{-/-}$***		
Lipids	**Vehicle** *(N=11)*	**ATL** *(N=8)*	**Vehicle** *(N=7)*	**ATL** *(N=6)*	
Cholesterol (mg/dL)	356.4±18.8	362.1±22.5	377.9±19.8	289.6±25.9	*NS*
Triglycerides (mg/dL)	123.6±13.1	86.1±5.1	107.8±5.3	114.1±7.3	*NS*
White blood cell count *(10^9/L)*	6.2±0.5	5.9±0.5	7.3±0.7	8.6±1.0	*NS*
Lymphocyte (%)	70.9±1.0	70.8±1.1	71.2±1.8	72.6±2.4	*NS*
Monocyte (%)	4.3±0.2	3.5±0.2	4.8±0.2	4.7±0.1	*NS*
Granulocyte (%)	24.5±0.9	25.6±1.0	23.9±1.8	22.6±2.4	*NS*
Body weight *(g)*	25.6±0.4	26.7±0.3	25.3±0.5	26.3±0.7	*NS*

ATL, Aspirin-triggered lipoxin A_4; *NS*, Non-significant (P>0.05; one way ANOVA)

Table 2: Lipid levels and white blood cell counts (mean±SEM) for either 16 (baseline) or 20 weeks old ApoE$^{-/-}$ x Fpr2$^{+/+}$ mice treated for 4 weeks with either Vehicle or ATL.

Lipids	**Baseline** *(N=5)*	**ATL** *(N=5)*	**Vehicle** *(N=5)*	
Cholesterol (mg/dL)	270.8±10.8	283.1±9.7	215.4±17.3	*NS*
Triglycerides (mg/dL)	108.1±9.01	106.6±4.7	77.7±11.8	*NS*
White blood cell count *(10^9/L)*	7.1±0.5	7.5±1.1	8.7±0.9	*NS*
Lymphocyte (%)	74.2±1.2	66.9±1.5	65.7±4.2	*NS*
Monocyte (%)	4.5±0.2	5.6±0.2	5.3±0.3	*NS*
Granulocyte (%)	21.2±1.1	27.5±1.5	28.9±3.9	*NS*
Body weight *(g)*	24.6±0.3	28.1±0.5*	27.8±0.7*	

ATL, Aspirin-triggered lipoxin A_4; *NS*, Non-significant (P>0.05; one way ANOVA), *P<0.05 vs. baseline

Table 3: Lipid levels and white blood cell counts (mean±SEM) for ApoE$^{-/-}$ x Fpr2$^{+/+}$ and ApoE$^{-/-}$ x Fpr2$^{-/-}$ on high fat diet for 4 weeks.

Lipids	**ApoE$^{-/-}$ x Fpr2$^{+/+}$** (N=8)	**ApoE$^{-/-}$ x Fpr2$^{-/-}$** (N=6)	
Cholesterol (mg/dL)	717.8±60.9	616.2±32.4	*NS*
Triglycerides (mg/dL)	149.3±9.6	145.2±14.9	*NS*
White blood cell count *(10^9/L)*	10.8±0.9	12.4±0.7	*NS*
Lymphocyte (%)	52.9±2.9	55.5±1.6	*NS*
Monocyte (%)	3.9±0.7	3.4±0.2	*NS*
Granulocyte (%)	43.1±3.0	41.1±1.6	*NS*

ATL, Aspirin-triggered lipoxin A_4; *NS*, Non-significant (P>0.05; Student's t-test)

Table 4. Cytokine and chemokine mRNA levels in the aorta derived from mice treated with either vehicle or ATL. Data (mean±SEM) expressed as $2^{-\Delta Ct}$.

	Aorta			*Spleen*		
	Vehicle *(N=11)*	ATL *(N=8)*	*P*	Vehicle *(N=11)*	ATL *(N=8)*	*P*
IFNγ	0.07±0.01	0.001±0.00	*<0.001*	0.03±0.00	0.01±0.00	*0.02*
TNF	0.28±0.10	0.05±0.01	*0.028*	2.12±0.12	1.19±0.08	*<0.001*
CCL2	0.77±0.17	0.29±0.04	*0.007*	0.43±0.02	0.29±0.04	*0.009*
CCL5	0.84±0.56	0.12±0.01	*NS*	6.75±0.27	4.62±0.29	*<0.001*
CXCL16	0.27±0.09	0.13±0.04	*0.021*	2.41±0.10	1.44±0.08	*<0.001*
IL-23a	0.78±0.76	0.01±0.01	*NS*	0.01±0.00	0.00±0.00	*0.016*

ATL, Aspirin-triggered lipoxin A_4; *NS*, Non-significant (P>0.05; Student's t-test)

Figure legends

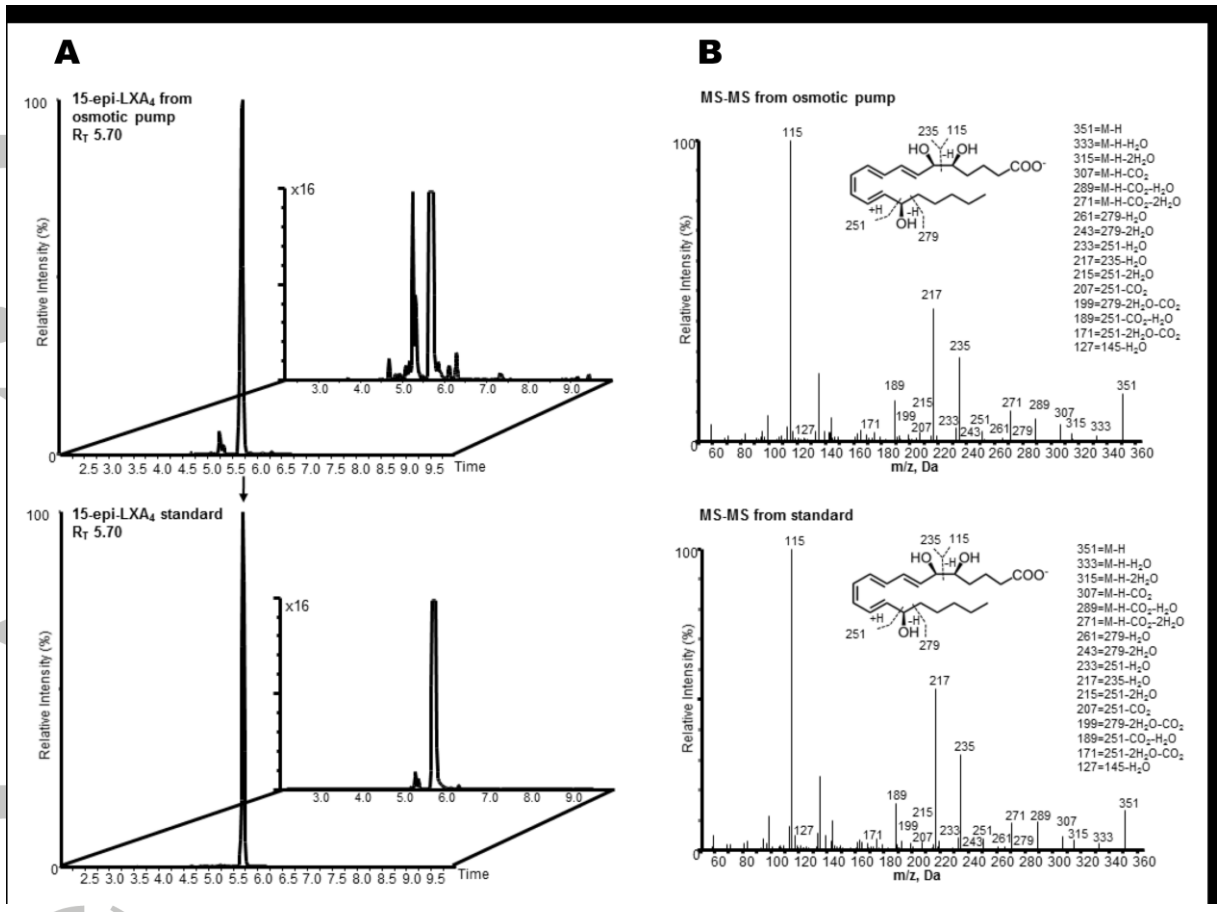

Fig 1 LC-MS-MS chromatograph of 15-epi-LXA_4 following incubation in osmotic pump. 15-epi-LXA_4 in PBS (237.5 ng in 200 uL) was added to an osmotic pump and incubated in PBS at 37˚C. After 4 weeks samples were placed in 2 volumes ice-cold MeOH and taken to solid phase extraction and LC-MS-MS. (a) Multiple reaction-monitoring (MRM) chromatograms of 15-epi-LXA_4 (m/z 351>115) from osmotic pump after 4 weeks (top) and 15-epi-LXA_4 standard (bottom; Inset: x16 magnification). (b) Accompanying MS-MS spectra of 15-epi-LXA_4 from osomotic pump incubation (top) and standard (bottom; inset: diagnostic ions; M, molecular mass).

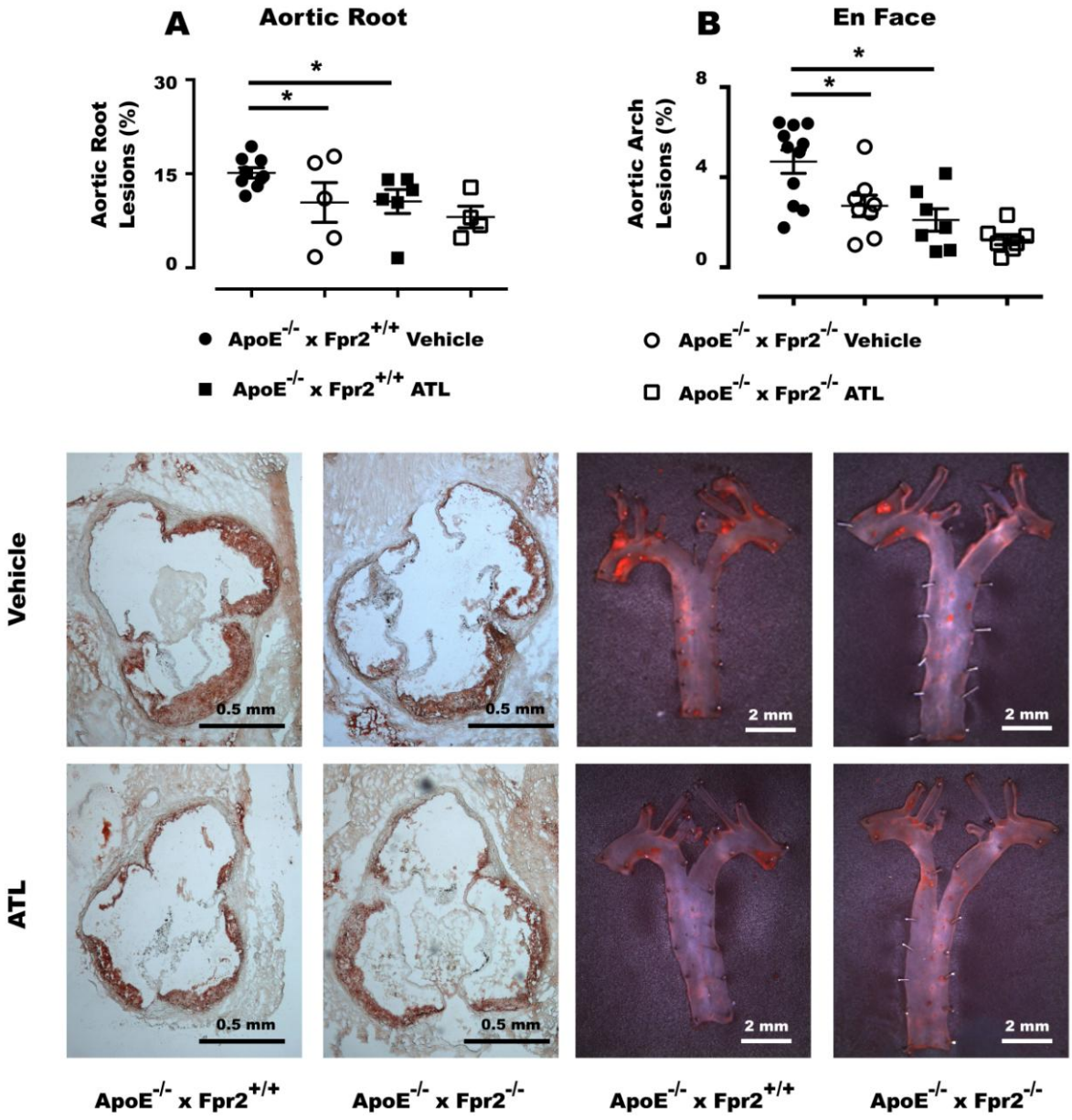

Fig 2 Atherosclerotic lesions in the aortic root (A) and *en face* analysis of the aortic arch (B) of 20 weeks old ApoE$^{-/-}$xFpr2$^{+/+}$ (filled symbols) and ApoE$^{-/-}$xFpr2$^{-/-}$ (open symbols) treated with either vehicle (circles) or ATL (squares) for 4 weeks. Below the graphs, representative micrographs of aortic root and *en face* stainings of each genotype and treatment are shown. At least N=6 in in each group as indicated and lines represent mean±SEM. *P<0.05.

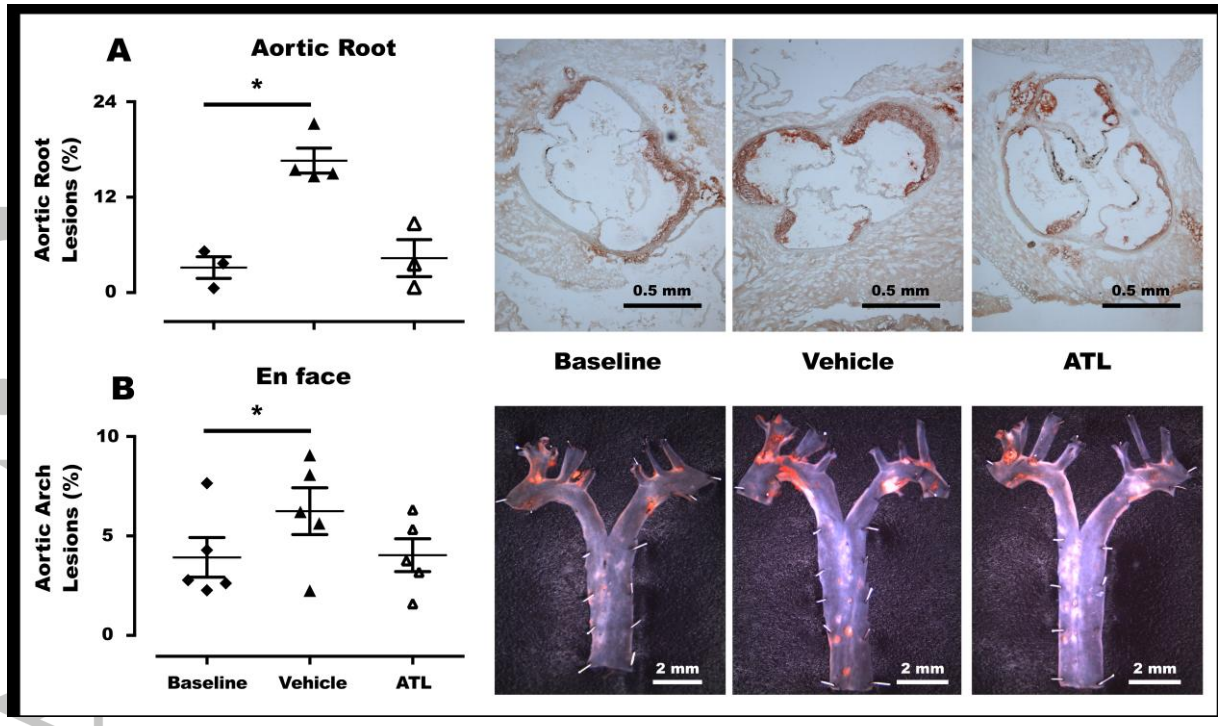

Fig 3. Atherosclerotic lesions in the aortic root and *en face* analysis of the aortic arch in ApoE$^{-/-}$xFpr2$^{+/+}$ mice at either 16 weeks (baseline, filled diamonds) or 20 weeks (triangles) after 4 weeks treatment with either vehicle (filled triangles) or ATL (open triangles). Representative micrographs of *en face* stainings of each group are also shown. At least N=5 in each group as indicated and lines represent mean±SEM. *P<0.05

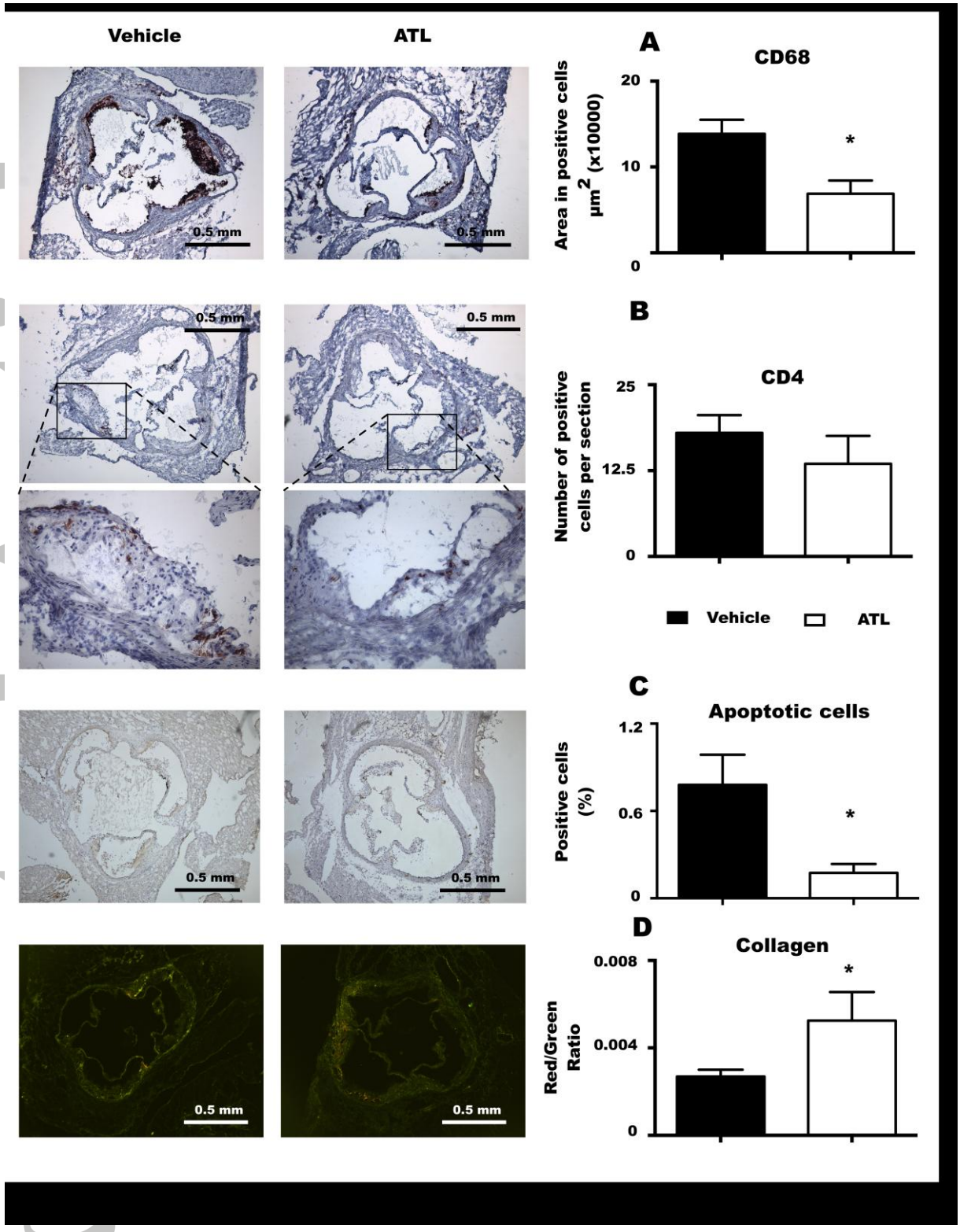

Fig 4. Plaque composition. Quantification of macrophages (CD68 positivity; A), T-lymphocytes (CD4 positivity; B), apoptotic cells (*in situ* apoptosis detection; C), and collagen fibers (Picrosirium red staining; D) in aortic roots of $ApoE^{-/-}xFpr2^{+/+}$ treated with either vehicle (black bars) or ATL (white bars). At least N=6 in all the experiments and bars represent mean±SEM. *P<0.05

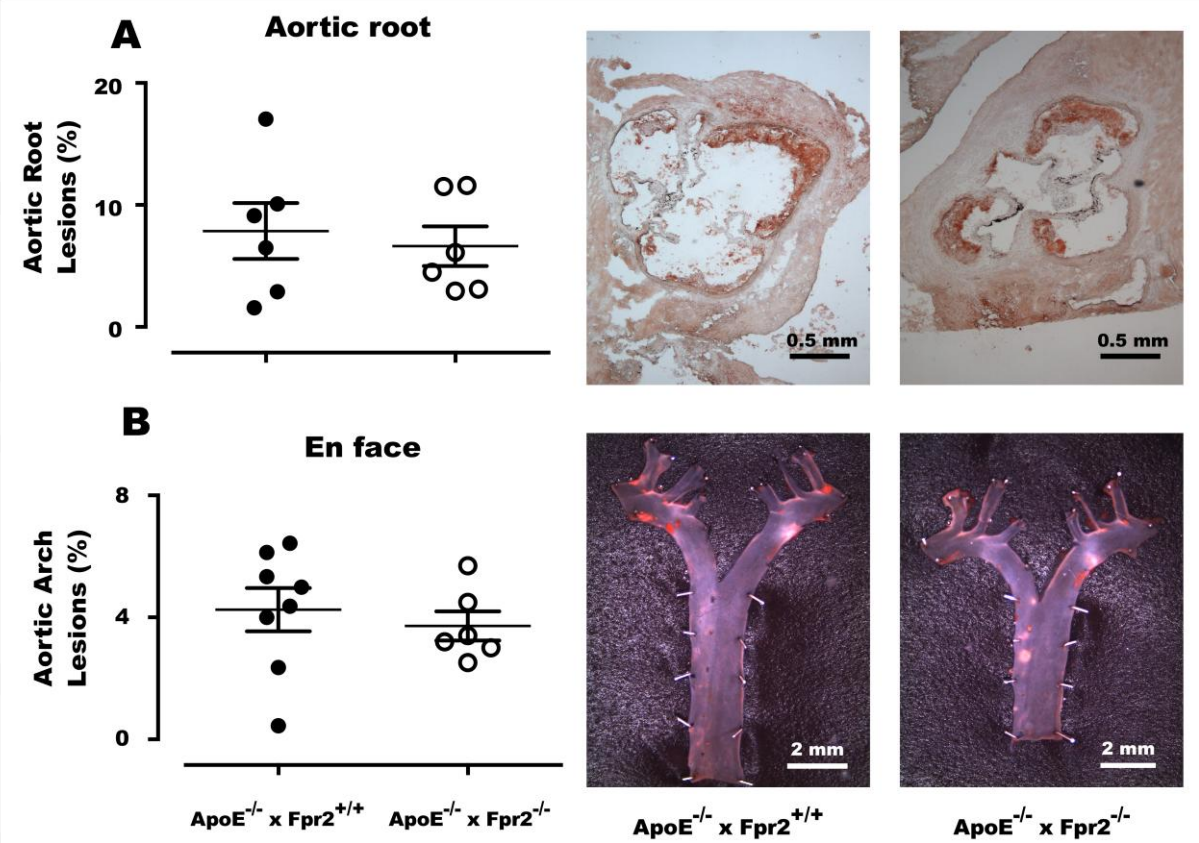

Fig 5. Atherosclerotic lesions in the aortic root (A) and *en face* analysis of the aortic arch (B) of 8 weeks old ApoE$^{-/-}$xFpr2$^{+/+}$ (filled circles) and ApoE$^{-/-}$xFpr2$^{-/-}$ (open circle) after 4 weeks of high fat diet. Next to the graphs, representative micrographs of aortic root and *en face* stainings of each genotype are shown. At least N=6 in each group as indicated and lines represent mean±SEM.

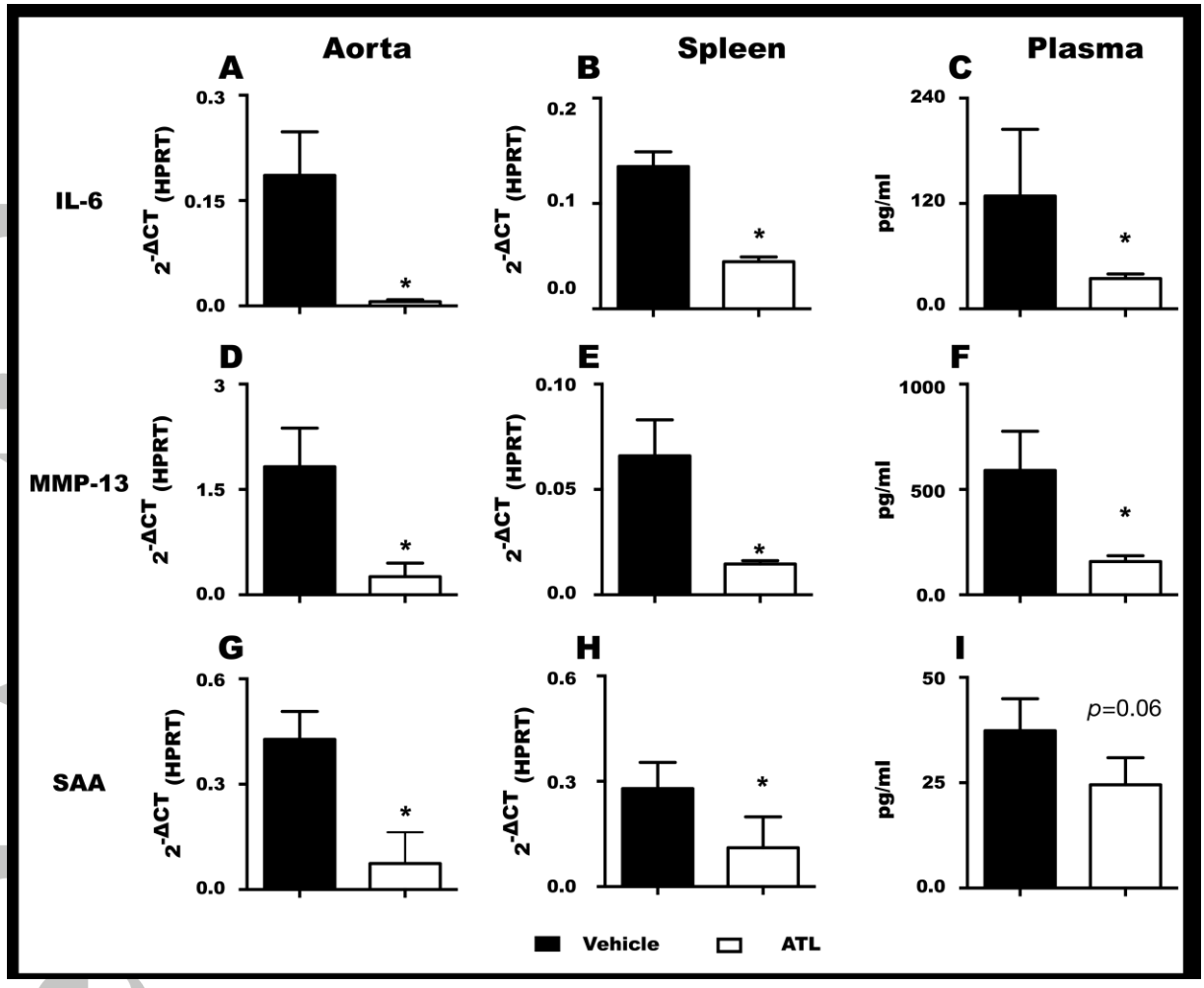

Fig 6. Effects of ATL treatment on IL-6 (A-C) and MMP-13 (D-F) and serum amyloid A (SAA; G-I) mRNA levels in the aorta (A, D, and G), and spleen (B, E, and H) and protein levels in plasma (C, F, and I). Data (mean±SEM) are expressed as either $2^{-\Delta CT}$ or pg/mL for at least N=6 in each group. *P<0.05.